J. Cent. South Univ. (2020) 27: 772−779
DOI: https://doi.org/10.1007/s11771-020-4330-1

Springer

Effect of oxalate on seed precipitation of gibbsite from sodium aluminate solution

YU Hai-yan(于海燕)[1, 2], ZHANG Bai-yong(张佰永)[2], PAN Xiao-lin(潘晓林)[1, 2], TU Gan-feng(涂赣峰)[1, 2]

1. Key Laboratory for Ecological Metallurgy of Multimetallic Mineral of Ministry of Education, Northeastern University, Shenyang 110819, China;
2. School of Metallurgy, Northeastern University, Shenyang 110819, China

Abstract: The precipitation performance and kinetics of gibbsite from sodium aluminate solution with different sodium oxalate concentrations as well as the corresponding influence mechanism of oxalate during the seed precipitation process were systematically investigated by physicochemical properties test, using SEM and Raman spectra. As the concentration of sodium oxalate increases, both the precipitation rate and particle size of gibbsite decrease. The presence of sodium oxalate not only increases the viscosity of sodium aluminate solution, but also promotes the transformation of $Al(OH)_4^-$ to $Al_2O(OH)_6^{2-}$. The overall reaction rate constant decreases and the apparent activation energy of gibbsite increases with the increasing sodium oxalate concentration, the rate controlling step of which is chemical reaction. The needle-like sodium oxalate precipitates on the gibbsite crystals and covers the active $Al(OH)_3$ seed sites, which leads to the lower precipitation rate and the finer particle size of gibbsite during the seed precipitation process.

Key words: sodium oxalate; sodium aluminate solution; gibbsite precipitation; kinetics; Raman spectra

Cite this article as: YU Hai-yan, ZHANG Bai-yong, PAN Xiao-lin, TU Gan-feng. Effect of oxalate on seed precipitation of gibbsite from sodium aluminate solution [J]. Journal of Central South University, 2020, 27(3): 772−779. DOI: https://doi.org/10.1007/s11771-020-4330-1.

1 Introduction

As significant impurities in the Bayer plant liquors, the effects of organic compounds which were mainly decomposed from bauxite during digestion on the Bayer process have been widely researched during the past decades [1−3]. Among all the organic compounds, oxalate was considered to be one of the most harmful impurities to the Bayer process, which increases the soda losses and impurity contents of the final alumina product, refines the granularity of precipitated gibbsite, and deteriorates the settling performance of bauxite residue as well as the scaling on the heating pipes [4, 5]. Therefore, lots of researches focused on the removal technologies of oxalate, including crystallization [6], oxidation [7], ion exchange [8], adsorption [9] and lime causticization [10]. KÖNIGSBERGER et al [11] developed several thermodynamic models to calculate the equilibrium solubility of oxalate in sodium aluminate solution. LOH et al [12] found that sodium oxalate is the main degradation product of organic compounds from the Bayer liquor by wet oxidation. LIU et al [13] and ZHANG et al [14] investigated the reaction behavior and removal mechanism of oxalate in sodium aluminate solution during the

Foundation item: Projects (51774079, 51674075) supported by the National Natural Science Foundation of China; Project (N182508026) supported by the Fundamental Research Funds for the Central Universities, China
Received date: 2019-09-15; **Accepted date:** 2019-11-28
Corresponding author: PAN Xiao-lin, PhD, Associate Professor; Tel: +86-24-83686460; E-mail: panxl@smm.neu.edu.cn; ORCID: 0000-0002-9814-0882

lime causticization process.

The seed precipitation of gibbsite ($Al(OH)_3$) from supersaturated sodium aluminate solution is one of the key steps in the Bayer process, which includes three crystallization processes, i.e. secondary nucleation, agglomeration and crystal growth [15−17]. Some researchers studied the co-precipitation mechanism of oxalate and gibbsite in synthetic sodium aluminate solution [18, 19], but the effects of oxalate on seed precipitation of gibbsite from sodium aluminate solution are still lack of systematic research. In this work, the precipitation rate and the particle size distribution of gibbsite during the seed precipitation process from synthetic sodium aluminate solution with different sodium oxalate concentrations were systematically investigated, and the corresponding precipitation kinetics and mechanism were also discussed.

2 Experimental

The gibbsite seeds used in this study were provided by Shandong Branch of China Aluminum Co., Ltd., and the other chemical reagents were of analytical grade purchased from National Pharmaceutical Group, China. Sodium aluminate solutions were prepared by dissolving $Al(OH)_3$ into heated NaOH solution at atmospheric pressure. The caustic alkali concentration of sodium aluminate solution for seed precipitation was 140 g/L (in form of Na_2O) and the molar ratio of Na_2O to Al_2O_3 was 1.4. The concentrations of sodium oxalate in sodium aluminate solutions were 0, 2, 4 and 6 g/L, respectively.

The seed precipitation experiments were carried out in batch tanks, the temperature of which was controlled by a thermostatical water bath. The sodium aluminate solutions were firstly added into the tanks, and then the calculated sodium oxalate was added to dissolve when the solution reached the predetermined temperature respectively. In order to simulate the two-stage decomposition process of industrial production, the gibbsite seeds with two different particle sizes were added into the preheated solution by two steps: 125 g/L at the beginning with the fine seeds, and then 400 g/L after 8 h with the coarse seeds. The particle size distributions of fine seeds and coarse seeds added to sodium aluminate solution are listed in Table 1. The

Table 1 Particle size distribution of gibbsite seeds added to sodium aluminate solution

Gibbsite seed	$D(0.1)$/μm	$D(0.5)$/μm	$D(0.9)$/μm
Fine seed	12.22	34.30	68.31
Coarse seed	29.37	71.78	139.76

precipitation experiments were carried out under the uniform cooling condition for 48 h. The initial precipitation temperatures were 55, 60, 65 and 70 °C respectively, while all the final precipitation temperatures were 50 °C.

The precipitation rate of gibbsite was calculated by the following equation:

$$\eta=(1-\alpha_0/\alpha_t)\times100\% \quad (1)$$

where α_0 and α_t are the molar ratio of caustic alkali to alumina in sodium aluminate solution before and after precipitation respectively.

The solutions after precipitation were determined by the volumetric method. The Raman spectra of sodium aluminate solution were obtained by a Raman spectroscopy (HR800) with the scanning wavenumbers from 200 to 1200 cm^{-1}. The viscosity of sodium aluminate solution was determined by the capillary method. The precipitated products were washed with hot deionized water and dried at 80 °C for 24 h. The morphology of precipitated products was observed by a field scanning electron microscope (SU8010). The particle size distribution of gibbsite was measured by a laser scattering mastersizer (Malvern 3000).

3 Results and discussion

3.1 Precipitation rate and particle size of gibbsite

The precipitation results of gibbsite from sodium aluminate solution with different sodium oxalate concentrations at different initial temperatures for different time are shown in Figure 1. All the precipitation rates of gibbsite increase with the increasing precipitation time. As seen from Figure 2, the precipitation rates of gibbsite increase with the decreasing temperature because of the relatively larger supersaturation at lower temperature, both in the presence and absence of sodium oxalate. However, at the same temperature, the precipitation rate of gibbsite decreases as the sodium oxalate concentration increases, which demonstrates that the presence of

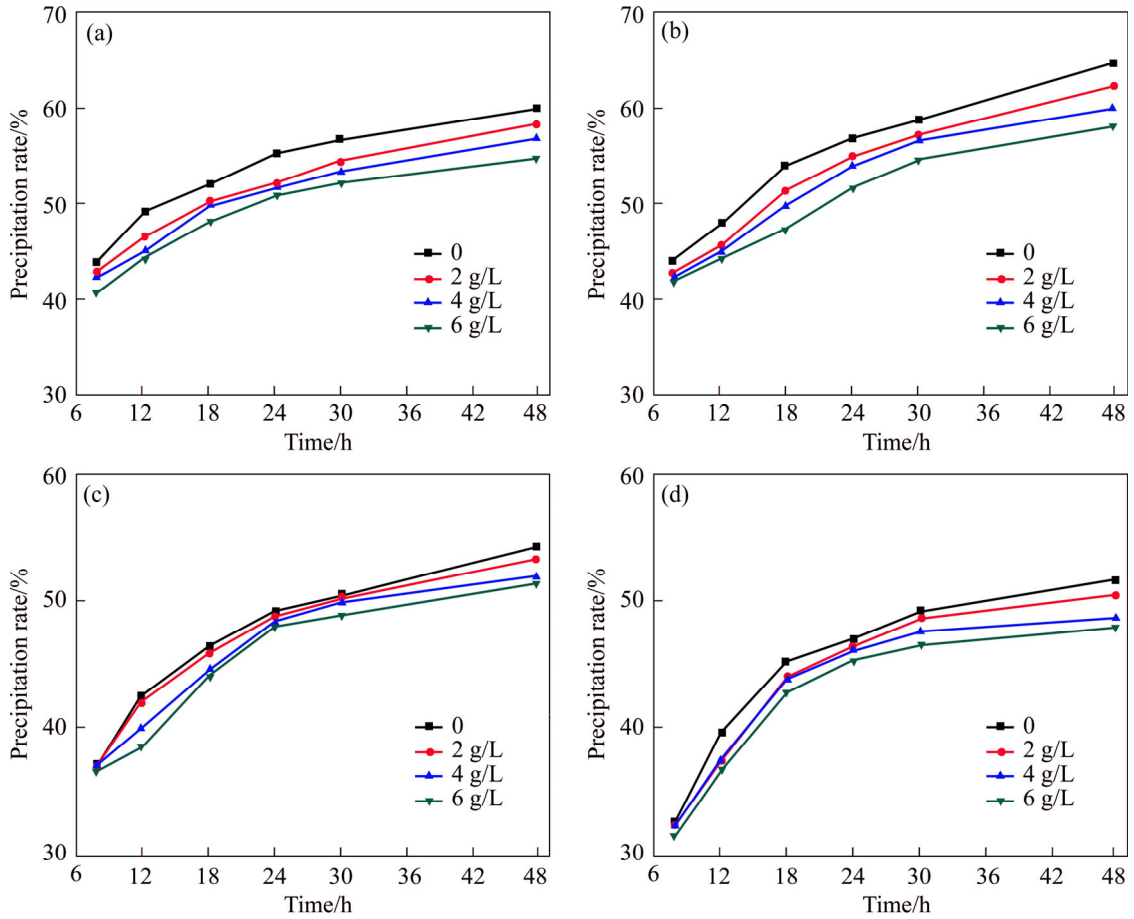

Figure 1 Precipitation rate of gibbsite from sodium aluminate solution at different initial temperatures: (a) 55 °C; (b) 60 °C; (c) 65 °C; (d) 70 °C

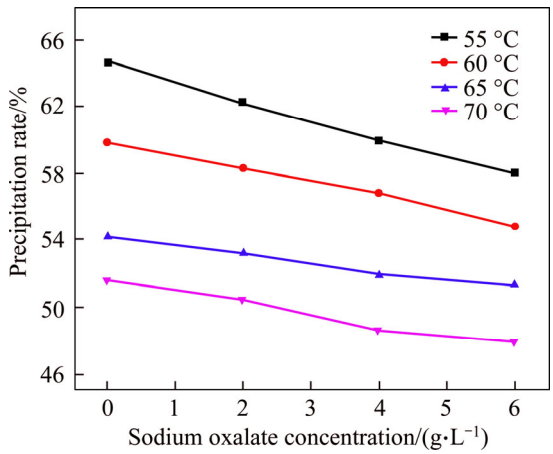

Figure 2 Precipitation rate of gibbsite from sodium aluminate solution with different sodium oxalate concentrations at different initial temperatures for 48 h

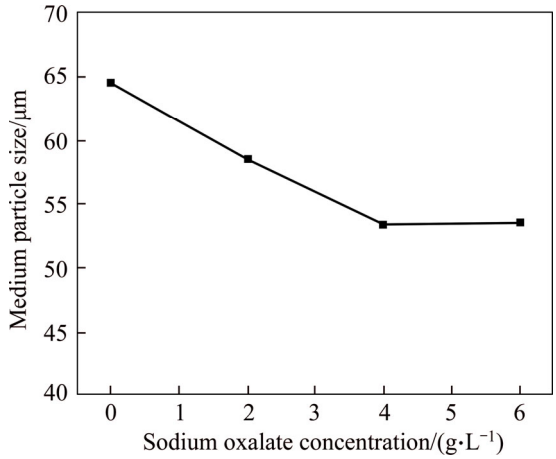

Figure 3 Medium particle size of gibbsite with different sodium oxalate concentrations at initial precipitation temperature 60 °C for 48 h

sodium oxalate reduces the final precipitation rate of gibbsite from sodium aluminate solution.

Figure 3 shows the medium particle size of gibbsite with different sodium oxalate concentrations when the initial precipitation temperature is 60 °C and the time is 48 h. As the sodium oxalate concentration increases, the particle size of gibbsite decreases at the final precipitation stage. The particle size results indicate that the presence of sodium oxalate hinders the crystal growth of gibbsite during the seed precipitation process.

3.2 Precipitation kinetics of gibbsite

The precipitation kinetics of gibbsite crystals depend on several factors, including solution supersaturation, reaction temperature, stirring rate, solid-liquor interface structure and impurities [17, 20]. The supersaturation of sodium aluminate solution is one of the most important factors, which directly influences the operations of crystallizer. The surface reaction was believed to be the controlling step and Eq. (2) given by MISRA et al [21] according to the power-law equations is the most classical for estimating the growth rate of gibbsite.

$$G=K_0\exp(-E/(RT))(C_A-C_{Ae})^2 \quad (2)$$

where C_A and C_{Ae} are the supersaturated and equilibrium concentrations of Al_2O_3, g/L; E is the growth activation energy of gibbsite crystals, J/mol; K_0 is the growth rate constant, m/h; G is the linear growth rate, μm/h.

According to the published equations for the linear growth rate of gibbsite, FARHADI et al [22] modified the linear growth rate equation, and concluded that the polynuclear model is the most probable mechanism for the surface growth of gibbsite crystals.

It is feasible to determine the main control step of seed precipitation by calculating the activation energy. Eq. (2) can be written as follows:

$$dC_A/dt=K(C_A-C_{Ae})^2 \quad (3)$$

where K is the overall reaction rate constant; t is the reaction time, h.

The equilibrium concentration of Al_2O_3 can be estimated from the empirical relation proposed by MISRA [23] for synthetic solutions as follows:

$$C_{Ae}=C_K\exp(6.2106-2486.7/T+1.0876C_K/T) \quad (4)$$

where C_K is the caustic alkali concentration of sodium aluminate solution (in form of Na_2O), 1/L; T is the thermodynamic temperature, K.

The plots of $1/(C_A-C_{Ae})$ versus t after seed precipitation from sodium aluminate solution with different sodium oxalate concentrations are shown in Figure 4. The overall reaction rate constants at different precipitation temperatures can be calculated by the slopes of curves, as listed in Table 2. Based on the reaction rate constants at

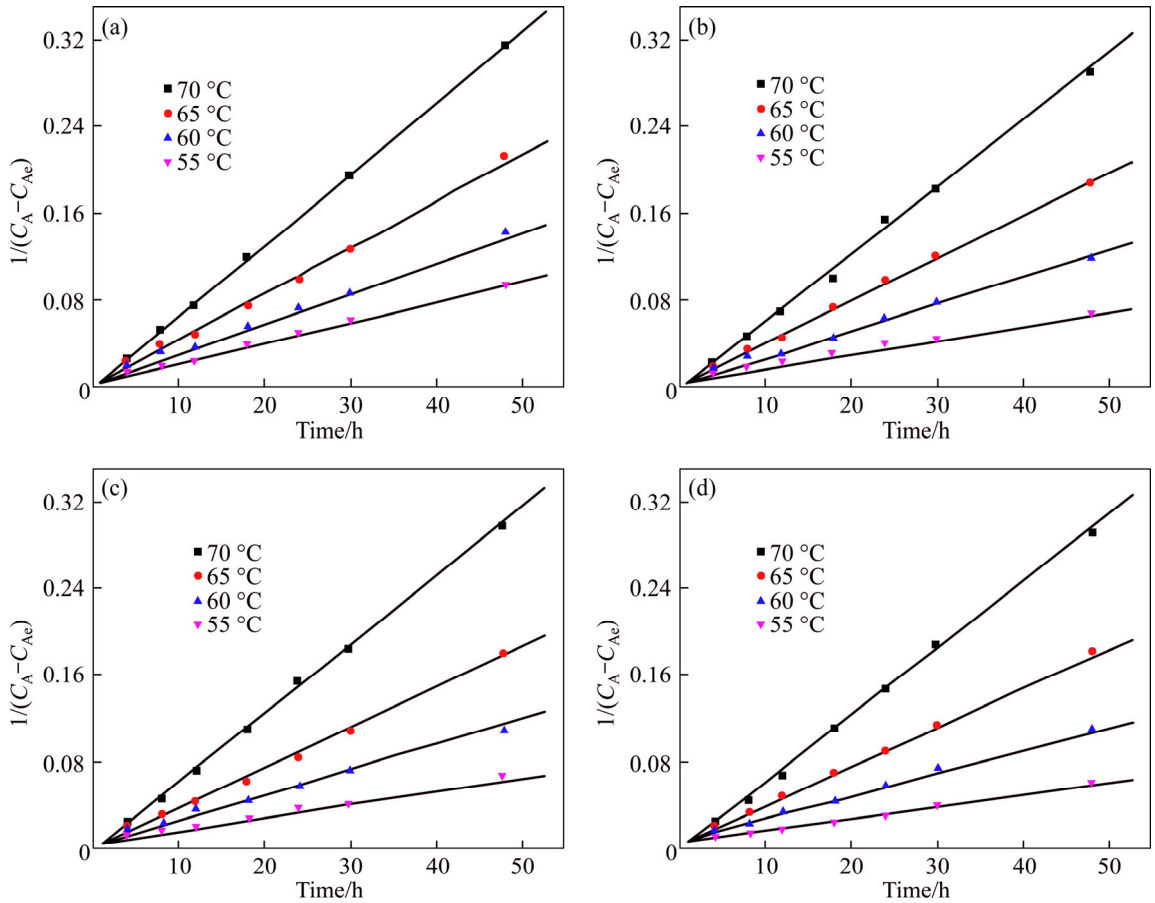

Figure 4 Relationship between $1/(C_A-C_{Ae})$ and t with different sodium oxalate concentrations: (a) 0 g/L; (b) 2 g/L; (c) 4 g/L; (d) 6 g/L

Table 2 Overall reaction rate constant (K) during seed precipitation at different initial temperatures with different sodium oxalate concentrations

Sodium oxalate concentration/(g·L^{-1})	Reaction rate constant			
	70 °C	65 °C	60 °C	55 °C
0	0.0019	0.0028	0.0043	0.0066
2	0.0013	0.0023	0.0039	0.0064
4	0.0012	0.0023	0.0037	0.0063
6	0.0011	0.0021	0.0036	0.0062

different initial temperatures, the apparent activation reaction energies with different sodium oxalate concentrations can be calculated according to the Arrhenius equation:

$$K=A\exp(-E/RT) \quad (5)$$

where A is the pre-exponential factor; E is the apparent activation energy, J/mol; R is the molar gas constant, 8.314 J/(mol·K); T is the reaction temperature, K. Thus, Eq. (5) can be transformed as follows:

$$\ln K=-E/(RT)+\ln A \quad (6)$$

The plots of reaction rate constants versus different initial temperatures are shown in Figure 5. Based on the slopes of curves, the apparent activation energies with different sodium oxalate concentrations were calculated according to Eq. (6), which are 77.8, 97.6, 102.9 and 107.1 kJ/mol when the sodium oxalate concentrations are 0, 2, 4 and 6 g/L, respectively. The apparent activation energy increases with the increasing sodium oxalate concentration. Furthermore, it can be concluded that the chemical reaction is the rate controlling step during the seed precipitation process.

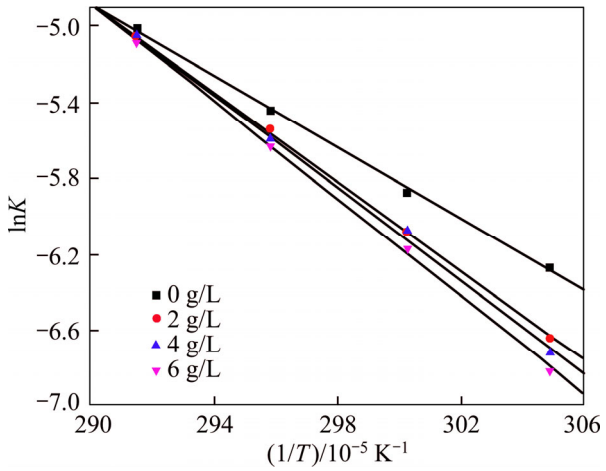

Figure 5 Relationship between ln$K$ and 1/T

3.3 Influence mechanism of oxalate

The gibbsite precipitation from sodium aluminate solution during the seed precipitation process is listed in Eq. (7). It shows that $Al(OH)_4^-$ is the main ion for the decomposition of sodium aluminate solution, which transforms into gibbsite during the seed precipitation process.

$$xAl(OH)_3+Al(OH)_4^-=(x+1)Al(OH)_3+OH^- \quad (7)$$

The Raman spectra of synthetic sodium aluminate solution with different sodium oxalat concentrations are shown in Figure 6. The peaks at 625 and 540 cm^{-1} belong to the vibrations of Al−OH bond in $Al(OH)_4^-$ tetrahedron and Al−O−Al bond in $Al_2O(OH)_6^{2-}$ dimer respectively [24], while the peak at 918 cm^{-1} belongs to the characteristic peak of $C_2O_4^{2-}$ [25]. The peak intensity of 540 cm^{-1} and the intensity ratio of 540 to 625 cm^{-1} gradually increase with the increase of sodium oxalate concentration, indicating that the amounts of $Al_2O(OH)_6^{2-}$ increase with the increasing sodium oxalate concentration. Therefore, the presence of sodium oxalate promotes the transformation of $Al(OH)_4^-$ to $Al_2O(OH)_6^{2-}$.

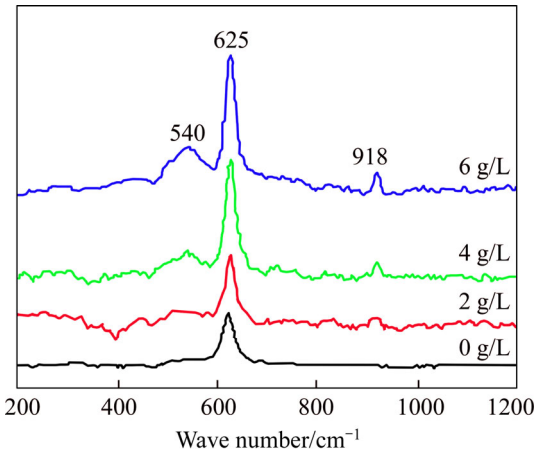

Figure 6 Raman spectra of sodium aluminate solution with different sodium oxalate concentrations

Figure 7 shows the viscosity of sodium aluminate solution with different sodium oxalate concentrations at different temperatures. The viscosity of sodium aluminate solution decreases greatly as the temperature increases. The presence of sodium oxalate increases the viscosity of sodium aluminate solution at the same temperature. As the sodium oxalate concentration increases, the polymerization degree of aluminate ions increases, which hinders the precipitation of gibbsite from sodium aluminate solution.

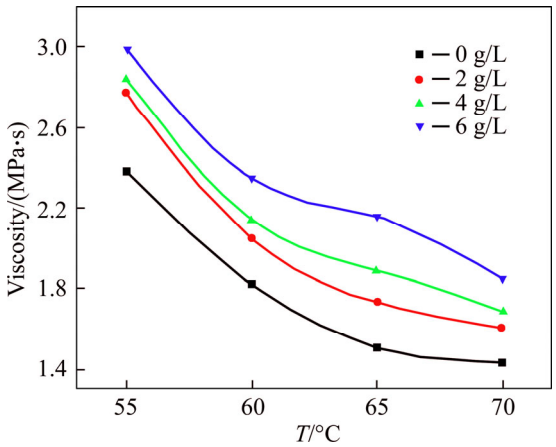

Figure 7 Viscosity of sodium aluminate solution with different oxalate concentrations at different temperatures

The morphologies of gibbsite precipitated from sodium aluminate solution without and with sodium oxalate are shown in Figures 8 and 9 respectively. The gibbsites precipitated from sodium aluminate solution without oxalate were found to be of agglomerates (Figure 8(a)), with well-formed hexagonal basal faces, prismatic faces and chamfered faces (Figure 8(b))

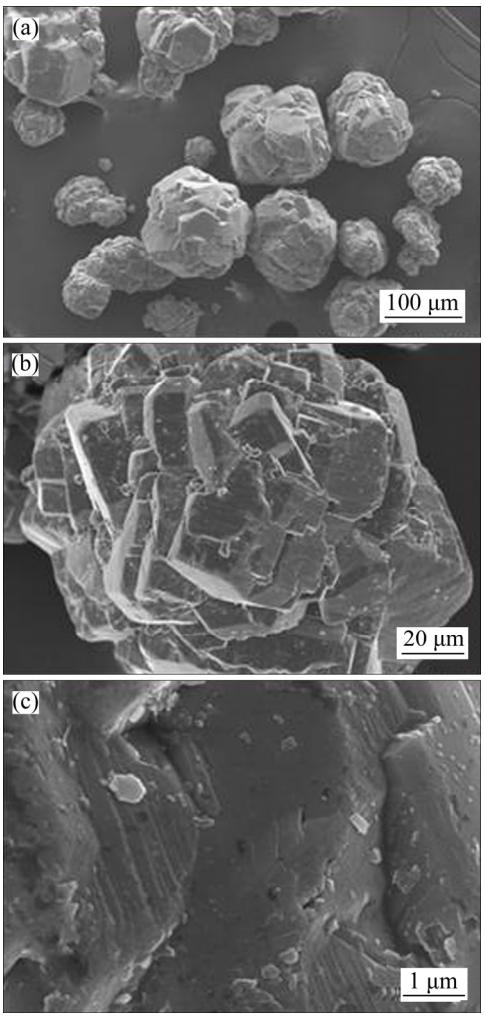

Figure 8 Morphology of gibbsite precipitated from sodium aluminate solution without oxalate

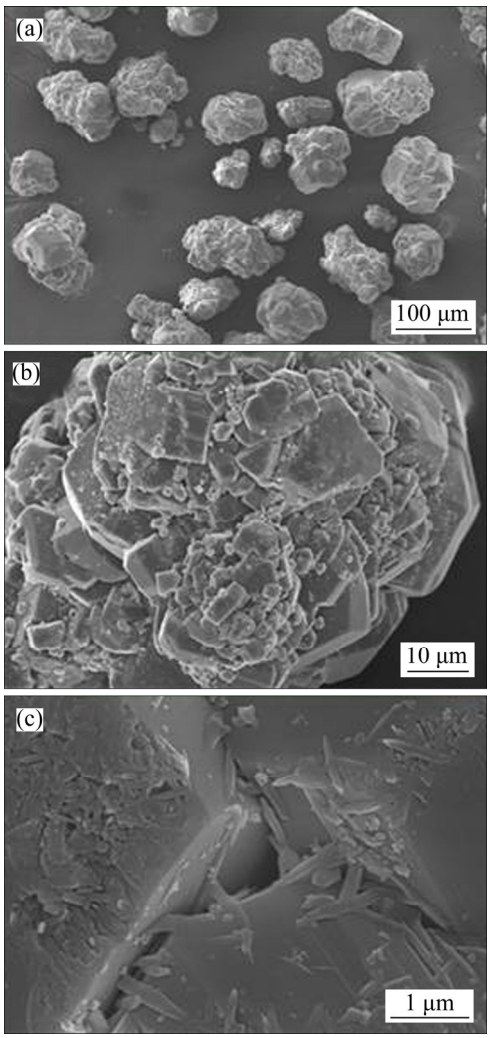

Figure 9 Morphology of gibbsite precipitated from sodium aluminate solution when sodium oxalate concentration is 6 g/L

The surface of gibbsite crystals is relatively smooth as shown in Figure 8(c). The particle size of gibbsite crystals precipitated from sodium aluminate solution with sodium oxalate is much smaller (Figure 9(a)) than those in Figure 8(a), which is consistent with the results in Figure 3. Meanwhile, the fine particles grown on the crystal faces of gibbsite (Figure 9(b)) are much more than those in Figure 8(b). The needle-like crystals referring to sodium oxalate were observed to precipitate on the gibbsite crystals, which is similar to FU's results [18].

According to the above results, the presence of sodium oxalate in sodium aluminate solution promotes the transformation of $Al(OH)_4^-$ to

$Al_2O(OH)_6^{2-}$, increases the corresponding viscosity of sodium aluminate solution and the apparent activation energy during the seed precipitation process, and thus decreases the precipitation rate of gibbsite. Meanwhile, as the precipitation process proceeds, sodium oxalate is precipitated with gibbsite, attached to the surface and covered some active sites of $Al(OH)_3$ seeds, which decreases the final particle size of precipitated products.

4 Conclusions

1) As the sodium oxalate concentration in sodium aluminate solution increases, both the precipitation rate and the final particle size of gibbsite decrease during the seed precipitation process.

2) The overall reaction rate constant decreases and the apparent activation energy of gibbsite increases with the increasing sodium oxalate concentration, and the chemical reaction is the rate controlling step.

3) The presence of sodium oxalate increases the viscosity of sodium aluminate solution, and promotes the transformation of $Al(OH)_4^-$ to $Al_2O(OH)_6^{2-}$.

4) The sodium oxalate with a needle-like morphology precipitates on the gibbsite crystals and covers the active $Al(OH)_3$ seed sites, which leads to the lower precipitation rate and the finer particle size of gibbsite.

References

[1] POWER G, LOH J, VERNON C. Organic compounds in the processing of lateritic bauxites to alumina. Part 2: Effects of organics in the Bayer process [J]. Hydrometallurgy, 2012, 127(18): 125−149. DOI: 10.1016/j.hydromet.2012.07.010.

[2] BUSETTI F, BERWICK L, MCDONALD S, HEITZ A, JOLL C A, LOH J, POWER G. Physicochemical characterization of organic matters in Bayer liquor [J]. Industrial & Engineering Chemistry Research, 2014, 53(15): 6544−6553. DOI: 10.1021/ie4028268.

[3] WANG Meng, HU Hui-ping, LIU Jin-wei, CHEN Qi-yuan. Negative effect of dissolved organic compounds on settling behavior of synthetic monominerals in red mud [J]. Journal of Central South University, 2016, 23(7): 1591−1602. DOI: 10.1007/s11771-016-3213-y.

[4] MAHMOUDIAN M, GHAEMI A, SHAHHOSSEINI S. Removal of carbonate and oxalate pollutants in the Bayer process using thermal and chemical techniques [J]. Hydrometallurgy, 2015, 154: 137−148. DOI: 10.1016/j.hydromet.2015.03.016.

[5] POWER G, LOH J S C, WAJON J E, BUSETTI F, JOLL C. A review of the determination of organic compounds in Bayer process liquors [J]. Analytica Chimica Acta, 2011, 689(1): 8−21. DOI: 10.1016/j.aca.2011.01.040.

[6] FU W, VAUGHAN J, GILLESPIE A, AROFF N M. Mechanisms of polyacrylate modified sodium oxalate crystallization from highly alkaline solutions [J]. Crystal Growth & Design, 2016, 16(3): 1519−1530. DOI: 10.1021/acs.cgd.5b01645.

[7] TARDIO J, BHARGAVA S, EYER S. Interactions between specific organic compounds during catalytic wet oxidation of Bayer liquor [J]. Industrial & Engineering Chemistry Research, 2004, 43(4): 847−851. DOI: 10.1021/ie030539g.

[8] HIND A R, BHARGAVA S K, GROCOTT S C. The surface chemistry of Bayer process solids: A review [J]. Colloids Surface A: Physicochemical & Engineering Aspects, 1999, 146(1): 359−374. DOI: 10.1016/S0927-7757(98)00798-5.

[9] PERROTTA A J, WILLIAMS F. Hydrocalumite formation in Bayer liquor and its promotional effect on oxalate precipitation [C]// Light Metals. Warrendale, Pennsylvania: TMS, 1995: 77−87.

[10] MOSTAFA M, AHAD G, SHAHROKH S. Removal of carbonate and oxalate pollutants in the Bayer process using thermal and chemical techniques [J]. Hydrometallurgy, 2015, 154(4): 137−148. DOI: 10.1016/j.hydromet.2015.03.016.

[11] KÖNIGSBERGER E, ERIKSSON G, MAY P M, HEFTER G. Comprehensive model of synthetic Bayer liquors. Part 1. Overview [J]. Industrial & Engineering Chemistry Research, 2005, 44 (15): 5805−5814. DOI: 10.1021/ie050024k.

[12] LOH J S C, BRODIE G M, POWER G. Wet oxidation of precipitation yield inhibitors in sodium aluminate solutions: Effects and proposed degradation mechanisms [J]. Hydrometallurgy, 2010, 104(2): 278−289. DOI: 10.1016/j.hydromet.2010.06.016.

[13] LIU Gui-hua, DONG Wen-bo, QI Tian-gui. Behavior of calcium oxalate in sodium aluminate solutions [J]. Transaction of Nonferrous Metals Society of China, 2017, 27(8): 1878−1887. DOI: 10.1016/S1003-6326(17)60212-7.

[14] ZHANG Bai-yong, PAN Xiao-lin, WANG Jiang-zhou, YU Hai-yan, TU Gan-feng. Reaction kinetics and mechanism of calcium oxide in dilute sodium aluminate solution with oxalate based on lime causticization [J]. Transactions of Nonferrous Metals Society of China, 2019, 29(6): 1312−1322. DOI: 10.1016/S1003-6326(19)65038-7.

[15] BEKKER A V, LI T S, LIVK I. Dynamic response of a plant-scale gibbsite precipitation circuit [J]. Hydrometallurgy, 2017, 170(7): 24−33. DOI: 10.1016/j.hydromet.2016.06.002.

[16] LI Xiao-bin, YE Pu-hong, ZHOU Qiu-sheng, LIU Jing-hui, PENG Zhi-hong, LIU Gui-hua, QI Tian-gui. Intensifying gibbsite precipitation from sodium aluminate solution by adding a mixed seed [J]. Journal of Central South University, 2019, 26(2): 312−322. DOI: 10.1007/s11771-019-4003-0.

[17] SANGWAL K. On the mechanism of crystal growth from solutions [J]. Journal of Crystal Growth, 1998, 192(1, 2): 200−214. DOI: 10.1016/S0022-0248(98)00424-2.

[18] FU W, JAMES V, ALISTAIR G. Aspects of the mechanism of nucleation and intergrowth of gibbsite crystals on sodium oxalate surfaces in concentrated alkaline solutions [J]. Crystal Growth and Design, 2015, 15(1): 374−383. DOI:

10.1021/cg501465v.

[19] FU W, JAMES V, ALISTAIR G. In situ AFM investigation of heterogeneous nucleation and growth of sodium oxalate on industrial gibbsite surfaces in concentrated alkaline solution [J]. Chemical Engineering Science, 2015, 126(4): 399−405. DOI: 10.1016/j.ces.2014.12.057.

[20] SANGWAL K. Growth kinetics and surface morphology of crystals grown from solutions: recent observation and their interpretations [J]. Progress in Crystal Growth and Characterization of Materials, 1998, 36(3): 163−248. DOI: 10.1016/S0960-8974(98)00009-6.

[21] MISRA C, WHITE E T. Crystallisation of Bayer aluminium trihydroxide [J]. Journal of Crystal Growth, 1971, 8(2): 172−178. DOI: 10.1016/0022-0248(71)90138-2.

[22] FARHADI F, MASOUD B B. Mechanism and estimation of $Al(OH)_3$ crystal growth [J]. Journal of Crystal Growth, 2002, 234 (4): 721−730. DIO: 10.1016/S0022-0248(01)01763-8.

[23] MISRA C. Solubility of aluminum trihydroxide (hydrargilite) in sodium hydroxide solution [J]. Chemical Engineering, 1970, 20: 619−628.

[24] PÁL S. The structure of Al(III) in strongly alkaline aluminate solutions—A review [J]. Journal of Molecular Liquids, 2009, 146: 1−14. DIO: 10.1016/j.molliq.2009.01.015.

[25] SUN Qiang. The Raman OH stretching bands of liquid water [J]. Vibrational Spectroscopy, 2009, 51: 213−217. DOI: 10.1016/j.vibspec.2009.05.002.

(Edited by FANG Jing-hua)

中文导读

草酸盐对铝酸钠溶液晶种分解过程氢氧化铝析出的影响

摘要：采用物化性能测定、扫描电镜和拉曼光谱等手段系统研究了晶种分解过程铝酸钠溶液不同草酸钠浓度下氢氧化铝的析出行为和动力学及其影响机理。随着铝酸钠溶液浓度的增加，氢氧化铝的析出率和晶粒尺寸均逐渐降低。草酸钠的存在不仅增加铝酸钠溶液的黏度，而且促进 $Al(OH)_4^-$ 向 $Al_2O(OH)_6^{2-}$ 的转变。随着草酸钠浓度的增加，氢氧化铝析出的反应速率常数降低，表观活化能增加，为化学反应控制。针状草酸钠在氢氧化铝晶体上析出，覆盖了活性晶种的位置，导致晶种分解过程中氢氧化铝分解率降低、晶粒细化。

关键词：草酸钠；铝酸钠溶液；氢氧化铝析出；动力学；拉曼光谱